

SEGMENT-LEVEL ATTRIBUTION FOR SELECTIVE LEARNING OF LONG REASONING TRACES

000
001
002
003
004
005 **Anonymous authors**
006 Paper under double-blind review
007
008
009
010

ABSTRACT

011 Large Reasoning Models (LRMs) achieve strong reasoning performance by gen-
012 erating long chains of thought (CoTs), yet only a small fraction of these traces
013 meaningfully contributes to answer prediction, while the majority contains repet-
014 itive or truncated content. Such output redundancy is further propagated after
015 supervised finetuning (SFT), as models learn to imitate verbose but uninformative
016 patterns, which can degrade performance. To this end, we incorporate integrated
017 gradient attribution to quantify each token’s influence on final answers and ag-
018 gregate them into two segment-level metrics: (1) *attribution strength* measures
019 the overall attribution magnitude; and (2) *direction consistency* captures whether
020 tokens’ attributions within a segment are uniformly positive or negative (high con-
021 sistency), or a mixture of both (moderate consistency). Based on these two metrics,
022 we propose a segment-level selective learning framework to identify important
023 segments with high attribution strength but moderate consistency that indicate
024 reflective rather than shallow reasoning. The framework then applies selective SFT
025 on these important segments while masking loss for unimportant ones. Experiments
026 across multiple models and datasets show that our approach improves accuracy
027 and output efficiency, enabling more effective learning from long reasoning traces.
028

1 INTRODUCTION

029
030 Recent Large Reasoning Models (LRMs) (Jaech et al., 2024; Guo et al., 2025; Yang et al., 2025)
031 have demonstrated strong capabilities in solving complex problems. Their effectiveness is largely
032 attributed to test-time scaling by increasing computation during inference to produce extended chains
033 of thought (CoT) (Wei et al., 2022) that include detailed problem understanding, step-by-step solution
034 processes, and comprehensive verification. These long-CoT trajectories have also become valuable
035 supervisory resources for cold-start supervised finetuning (SFT) (Muennighoff et al., 2025).
036

037 However, current reasoning CoTs often span thousands of tokens, of which only a small fraction
038 meaningfully contributes to reaching the correct answer or improving confidence (Sui et al., 2025).
039 A substantial portion consists of redundant repetition or incomplete truncated thoughts (Wang
040 et al., 2025d), as illustrated in Fig. 1 (left). More critically, verbosity without substance actively
041 degrade reasoning performance as CoT length increases (Wu et al., 2025; Huang et al., 2025). This
042 phenomenon is also evident by the right-top panel of Fig. 1 where incorrect CoTs are typically
043 correlated with more segments and tokens than correct CoTs for the same queries. Training LLMs on
044 verbose CoT supervision with sparse positive contribution further exacerbates these issues. Models
045 learn to imitate redundant behaviors, waste learning capacity on trivial continuations, and fail to
046 prioritize the crucial high-impact parts of reasoning sequences Lin et al. (2024). As a result, finetuned
047 models tend to achieve limited accuracy gains and generate inefficient outputs.

048 Prior studies have explored various strategies to identify important parts in long reasoning chains to
049 construct compressed CoT supervision for efficiency purposes. However, they either focus on fine-
050 grained token-level analysis (Xia et al., 2025b) that neglects semantic integrity and fails to interpret
051 redundancy in terms of meaningful reasoning units, or rely on segment-level perplexity (Cui et al.,
052 2025a) or entropy (Li et al., 2025b) calculations. These indirect metrics provide not entirely consistent
053 signals of importance and are prone to both false positives and false negatives. False positives occur
when methods overemphasize superficial scaffolding text (e.g., “So, let’s calculate step by step”) that
contributes little to actual reasoning yet serves as linguistic bridges whose removal disrupts

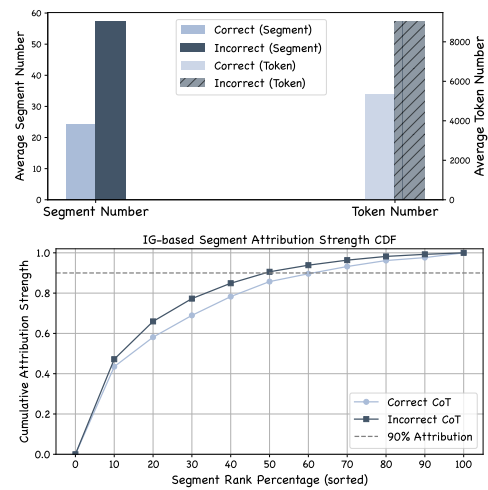
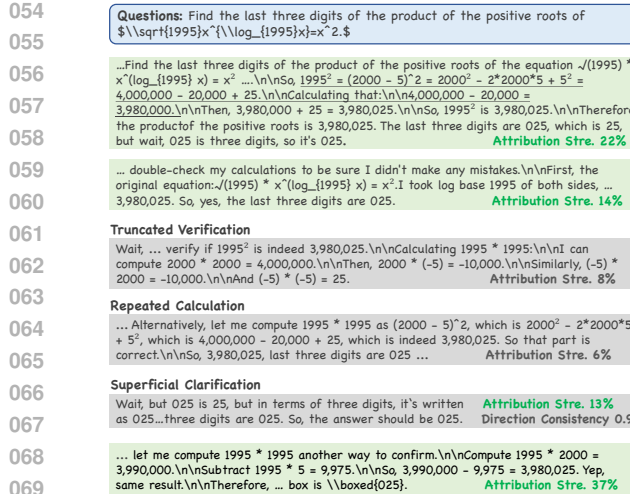


Figure 1: **Left:** An illustrative CoT with important (green blocks) and redundant segments (gray blocks). Our metrics distinguish important from redundant segments (repetitions, truncations, superficial clarifications) with low strength and extremely high consistency. “Attribution Stre.” denotes normalized strength across all segments. **Right-top:** Segment and token counts in correct vs. incorrect CoTs for the same queries. **Right-bottom:** Cumulative distribution function (CDF) of normalized segment strength in correct and incorrect CoTs, with segment ordered in descending strength.

subsequent textual coherence. False negatives arise when methods filter out independent verification or intermediate conclusions that, while exhibiting low-entropy and their removal not affecting linguistic fluency, significantly enhance the probability of reaching correct final answers. Consequently, existing methods cannot accurately and comprehensively distinguish truly important segments from various forms of redundant content that meaninglessly contribute to reasoning accuracy.

In this work, we systematically identify important segments that directly contribute to correct answer prediction within long CoTs, and show that unimportant segments cluster into distinctive redundant patterns. Specifically, we utilize integrated gradient (IG) attribution (Sundararajan et al., 2017) to calculate each token’s direct influence on improving correct answer prediction and aggregate token-level attributions at the segment level to obtain two metrics: (1) *Attribution strength* quantifies the overall magnitude of a segment’s influence on the model’s prediction by summing absolute IG values within each segment with length normalization. (2) *Attribution direction consistency* is defined as the ratio between the absolute sum of signed IG attributions and the sum of absolute IG attributions, captures how uniformly a segment contributes in one direction (either positively or negatively toward the correct answer). Extremely high consistency often reflects shallow reasoning, such as segments with uniformly positive token IGs but serve as superficial clarification (see the penultimate segments in Fig. 1 left). In contrast, moderate consistency indicates more reflective reasoning that mixes supportive and corrective attribution within a segment, which is more critical for problem solving.

We first verify significant redundancy in long CoTs using *attribution strength*, showing that 30~40% of segments accumulate over 80% of total attribution in both correct and incorrect CoTs (Fig. 1, right-bottom). Building on this insight, we propose a segment-level selective learning framework that learns the most critical parts of long CoTs leveraging *attribution strength* and *direction consistency*. It identifies segments with high strength but moderate consistency as important, filtering out redundancies like repeated content, truncated thoughts, and dispensable clarifications with minimal gains on correct answer probability. Unlike pruning-based SFT methods that compress CoT supervision but compromise accuracy, our framework applies selective SFT (Lin et al., 2024) that trains only on important segments while masking loss for unimportant ones. This acts as implicit regularization by preventing overfitting to uninformative content. Experiments across multiple models and datasets, using both self-generated and reference long CoTs, show that our method outperforms full-CoT SFT by improving reasoning efficacy (up to 4.7%) while reducing output length (up to 18%). Notably, our important segment identification can be broadly applied to other contexts, such as emphasizing policy gradient updates on important content in reinforcement learning.

108

2 METHODOLOGY

109

2.1 PRELIMINARY

110 A long-form CoT typically comprises multiple segments, each focusing on distinct aspects such as
 111 detailed problem understanding, intermediate reasoning exploring different solutions, or multiple
 112 verification process. Moreover, it inevitably contains redundant content, including repeated or
 113 truncated thought, and excessive clarification of self-evident facts, which diminishes the overall
 114 quality and efficiency of the CoT. To facilitate segment-level importance analysis of long CoTs,
 115 we first partition each long CoT T into multiple segments $T = \{S_1, S_2, \dots, S_n\}$ using common
 116 transition keywords (e.g., “\n\nWait”, “\n\nAlternatively”) that naturally occur within reasoning
 117 traces, following (Lu et al., 2025). The complete list of segmentation keywords is in the Appendix C.2.
 118

119 **Importance Definition** We define a segment within the full reasoning trace as important if it
 120 contributes to the final answer prediction, either by guiding transition from incorrect to correct
 121 answers or by enhancing confidence of correct answers. An intuitive approach is to sequentially
 122 append segments and force answer generation when adding each new segment to compute the change
 123 in correct answer probability as its attribution. However, this method underestimates segments that
 124 contribute indirectly, such as problem understanding or exploration of incorrect alternatives, which
 125 may not immediately improve answer prediction but establish crucial foundations for subsequent
 126 reasoning steps. Leave-one-out methods that mask individual segments and measure their effect on
 127 the final prediction, suffer from the same limitation, as omitting these segments typically does not
 128 significantly alter final answer prediction when their subsequent content remains intact. Therefore,
 129 we adopt a more principled approach using integrated gradients (IG) (Sundararajan et al., 2017) to
 130 measure each segment’s attribution to the final answer prediction.
 131

132

2.2 INTEGRATED GRADIENTS BASED SEGMENT IMPORTANCE

133 IG measures input token attribution by computing partial derivatives of the model output with respect
 134 to each input feature along a straight-line interpolation path from an uninformative baseline to the
 135 actual input embedding. By accumulating gradients across all interpolated points, IG estimates
 136 the total attribution of each input token to the final prediction. This approach captures both direct
 137 and indirect influences, making it particularly suitable for identifying the importance of reasoning
 138 segments that may contribute implicitly rather than immediately affecting the final answer prediction.
 139

140 Formally, given a model F , an input token embedding x and its baseline value x' (typically the
 141 padding token embedding), the integrated gradient for the i -th input dimension is formulated as
 142

$$143 \text{IG}_i(x) = (x_i - x'_i) \times \int_{\alpha=0}^1 \frac{\partial F(x' + \alpha \cdot (x - x'))}{\partial x_i} d\alpha \quad (1)$$

$$145 \approx (x_i - x'_i) \times \frac{1}{J} \sum_{j=1}^J \frac{\partial F(x' + j/J \cdot (x - x'))}{\partial x_i} \quad (2)$$

148 where x_i and x'_i refer to the i -th dimension of x and x' , respectively. The integral is approximated
 149 using J interpolation steps where j denotes the j -th step.
 150

151 **Segment-level Aggregation** After computing IG attribution of each input token as $\text{IG}(x) = \sum_i \text{IG}_i(x)$, we aggregate them at the segment level to obtain segment-wise importance scores. While
 152 IG values can be either positive or negative, where positive values indicate increased likelihood of
 153 predicting the correct answer and negative values indicate a decrease, tokens with negative IG values
 154 should not be dismissed as unimportant. Negatively attributed tokens may represent incorrect but
 155 necessary exploratory reasoning that ultimately guides the model toward the correct solution. For
 156 example, initial segments often exhibit overall negative IG sums, but these segments are typically
 157 important for establishing problem understanding and initial exploration. Therefore, we utilize the
 158 absolute IG value of each token to capturing the magnitude of influence regardless of direction.
 159

160 We aggregate the absolute IG values for all tokens within each segment and define two segment-level
 161 measures: (1) Attribution Strength: computed as the sum of absolute IG values within the segment
 with square root length normalization applied to prevent bias toward longer segments; (2) Attribution

162 Direction Consistency: measures the extent to which a segment exhibits consistent positive or negative
 163 contributions versus internally conflicting mixed attributions.

164 Formally, given a segment $S = \{o_1, \dots, o_N\}$ with N tokens, where each token o_n is associated with
 165 an IG value $IG(o_n)$, we define the segment-level attribution strength and direction consistency as:

$$167 \text{Strength}(S) = \frac{\sum_{o_n \in S} |IG(o_n)|}{\sqrt{N}}, \text{Consistency}(S) = \frac{|\sum_{o_n \in S} IG(o_n)|}{\sum_{o_n \in S} |IG(o_n)|}. \quad (3)$$

170 To ensure strength comparability across all segments within a CoT, we further normalize all strength
 171 scores across the set of segments $\{S_1, S_2, \dots, S_M\}$. Specifically, for each segment S_m , the normal-
 172 ized attribution strength is defined as

$$173 \text{Strength}'(S_m) = \frac{\text{Strength}(S_m)}{\sum_{j=1}^M \text{Strength}(S_j)}. \quad (4)$$

176 2.3 SEGMENT-LEVEL SELECTIVE LEARNING

178 **Important Segment Identification** We utilize our segment-level metrics to distinguish critical
 179 segments from unimportant ones for more targeted learning of long CoTs. Important segments should
 180 exhibit higher attribution strengths that occupy a substantial portion of total attribution across all
 181 segments, and moderate rather than extremely high attribution direction consistency. **Extremely**
 182 **consistent attribution directions (most positive or most negative) may indicate shallow reasoning (e.g.,**
 183 **dispensable explanation of final answers or uninformative exploration, as analyzed in Appendix A)**
 184 while moderate consistency often reflect reflective and critical reasoning patterns where the model
 185 explores different possibilities, refines its understanding, and eliminates incorrect content, which are
 186 more valuable for learning effective reasoning strategies. Specifically, given a CoT with segments
 187 $\{S_1, S_2, \dots, S_M\}$, we first rank segments in descending order of their normalized attribution strength.
 188 Let π be a permutation such that:

$$189 \text{Strength}'(S_{\pi(1)}) \geq \text{Strength}'(S_{\pi(2)}) \geq \dots \geq \text{Strength}'(S_{\pi(M)}) \quad (5)$$

190 We then identify the minimal number of top-ranked segments k^* whose cumulative attribution exceeds
 191 a predefined threshold τ (e.g., 80%):

$$193 k^* = \arg \min_{k \in 1, 2, \dots, M} \left\{ \sum_{i=1}^k \text{Strength}'(S_{\pi(i)}) \geq \tau \right\} \quad (6)$$

195 Finally, we define the important segment set as those among the top- k^* segments whose attribution
 196 direction consistency is below a threshold β (e.g., 0.8), while the remaining as unimportant ones.

$$198 \mathcal{S}_{\text{important}} = \{S_{\pi(i)} \mid i \leq k^*, \text{Consistency}(S_{\pi(i)}) \leq \beta\} \quad (7)$$

200 **Selective SFT** Long-CoT trajectories serve as valuable supervisory resources for cold-start of
 201 reasoning models via SFT, which optimizes parameters θ using the cross-entropy loss over all tokens.

$$202 L_{\text{SFT}}(\theta) = -\frac{1}{T} \sum_{t=1}^T \log P(o_t | o_{<t}, q; \theta) \quad (8)$$

205 where T denotes the length of the reasoning trajectory, o_t is the predicted token at position t ,
 206 $o_{<t} = \{o_1, o_2, \dots, o_{t-1}\}$ represents the preceding token sequence, and q is the input query.

207 To mitigate learning from meaningless parts, prior efficiency works mainly prune redundant portions
 208 of each complete CoT, yielding more concise supervision, but pruning typically degrades performance.
 209 Instead, we follow (Lin et al., 2024) and propose to selectively train only on tokens within important
 210 segments. This strategy ensures that parameter updates are driven solely by the most critical reasoning
 211 parts, while preserving coherence of the full trajectory. The selective SFT loss is formulated as:

$$213 L_{\text{Selective-SFT}}(\theta) = -\frac{1}{\sum_t I(o_t)} \sum_{t=1}^T I(o_t) \log P(o_t | o_{<t}, q; \theta) \quad (9)$$

215 where $I(o_t)$ indicating whether token o_t belongs to a segment S_m with $S_m \in \mathcal{S}_{\text{important}}$.

216 **3 SEGMENT IMPORTANCE ANALYSIS**

218 Before applying our segment-level selective learning strategy, we first validate that our importance
 219 metric effectively distinguishes meaningful reasoning parts from redundant behaviors and determine
 220 the optimal hyperparameters τ and β .

221 **Analysis Setup** We conduct an investigation on self-generated long reasoning trajectories from
 222 the LIMO datasets (Ye et al., 2025) using R1-Distill-Qwen2.5-7B (Guo et al., 2025). From 32
 223 candidate samples per problem, we select the shortest correct and incorrect outputs, split them
 224 into segments and compute their attribution strength and consistency. Segments are ranked as Eq. 5,
 225 with cumulative attribution averaged across percentage intervals, as illustrated in the top-right part of
 226 Fig. 1. The analysis reveals that only 30%~40% of segments contribute significantly (80%) to the
 227 final prediction, regardless of correctness, while most segments exhibit low attribution. This verifies
 228 substantial redundancy in long CoTs and motivates our approach for identifying important segments.
 229

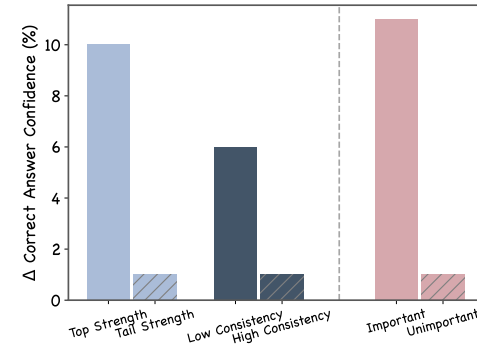
230 **3.1 IMPORTANT VERSUS UNIMPORTANT SEGMENTS**

231 We aggregate important and unimportant segments, respectively from all correct reasoning outputs¹
 232 and compare the distinct patterns exhibited by these two subsets. We first intuitively set the threshold
 233 $\tau = 80\%$, $\beta = 0.95$ as Eq. 6, 7 for this comparative analysis.

234 **1. Important segments yield greater improvement in correct answer predictions.** We sequentially append segments to the input and enforce answer generation after adding each new segment to compute the change Δ in correct answer confidence relative to without that segment. The model's confidence on the correct answer is defined as the probability that it generates the correct answer. We empirically estimate this correct answer confidence by calculating the fraction of multiple temperature-sampled generations (i.e., 32 samples) that produce the correct answer. As shown in Fig. 2, segments with higher attribution strength (top 80% of total attribution), and moderate direction consistency achieve significantly larger gains in correct answer confidence compared to their counterparts. This suggests that segments with high strength but moderate consistency reflect the critical exploratory reasoning that contribute to accurate predictions.

235 **2. Important segments exhibit relatively lower perplexity and entropy.** We calculate the log
 236 perplexity and entropy of all tokens in each long reasoning trace and aggregate them at the segment
 237 level to compare the linguistic properties between important and unimportant segments. As shown
 238 in Fig. 3, important segments consistently exhibit significantly lower log perplexity and entropy
 239 compared to unimportant segments. This indicates that our identified critical segments tend to be more
 240 predictable and carry lower uncertainty, likely reflecting processes such as problem understanding,
 241 logical deduction or essential computations that follow more constrained patterns. In contrast,
 242 unimportant segments, such as incomplete truncations associated with higher uncertainty (Wang et al.,
 243 2025d), as well as verbose explanations or dispensable elaborations that exhibit higher variability and
 244 greater linguistic freedom, resulting in higher perplexity and entropy.

245 **3. Unimportant segments are more characterized by repetition or incomplete truncation.** We
 246 further examine whether unimportant segments are closely associated with redundant reasoning
 247 behaviors such as repetition and incomplete truncation. To this end, we calculate BLEU similarity
 248 of each segment against all preceding segments within the same CoT (rightmost panel, Fig.3).
 249 Unimportant segments exhibit overall higher BLEU similarity scores compared to important segments.
 250 In particular, unimportant segments contain substantially more highly repetitive content (e.g., BLEU
 251 > 0.8) that reiterate previously established reasoning. In addition, we prompt Qwen3-8B (Yang
 252 et al., 2025) to assess whether each segment is incompletely truncated, meaning that subsequent
 253



254 Figure 2: Change (Δ) in correct answer confidence across different segment types.

255 ¹We focus on correct reasoning outputs, as our objective is to leverage reliable reasoning traces for SFT.

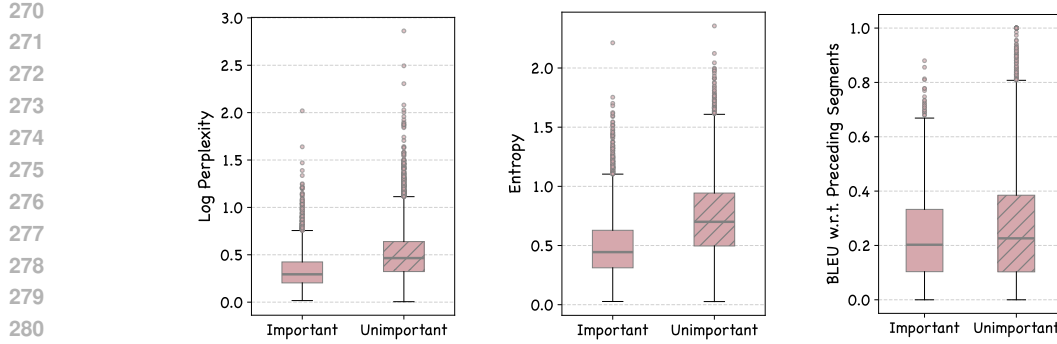


Figure 3: Log perplexity, entropy and BLEU similarity of important versus unimportant segments.

segments failing to logically follow it (as implemented in Appendix B). The results show that 49% of unimportant segments are classified as truncated compared with only 26% of important segments. These results demonstrate that unimportant segments identified by our method are more strongly associated with repetition and truncation, contributing minimal additional value to the reasoning chain and can even introduce noise that obscures the logical flow. We additionally analyze the positional distribution of important versus unimportant segments within each CoT in Appendix A.

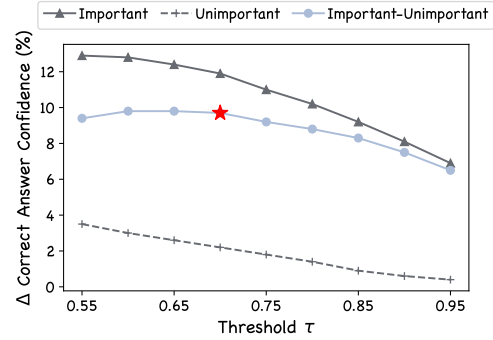
3.2 HYPERPARAMETER SEARCH

To determine the optimal threshold τ for identifying high-impact segments for targeted training, we adopt a greedy search strategy by selecting τ^* that maximizes the difference in correct answer confidence change Δ between resulted important and unimportant segments while minimizing false negatives (i.e., ensuring that unimportant segments exhibit the lowest confidence gain). As shown in Fig. 4, we set the optimal threshold as $\tau = 0.7$. On average, this setting yields about 33% of segments classified as important, accounting for 45% of the tokens within each self-generated CoT. This imbalance is because important segments tend to be longer, whereas unimportant ones often either repeat part of the previous content or are prematurely truncated in the middle. We further ablate different values of β under $\tau = 0.7$ and provide experimental comparison of varying τ on overall performance in Appendix D and identify $\beta = 0.8$ as the optimal consistency threshold.

4 EXPERIMENTS

4.1 SETUP

Training Details We compare our selective SFT on IG-based important segments against standard SFT on full long CoT supervision, experimenting both instruction-following and reasoning baseline models of different scales: R1-Distill-Qwen2.5-1.5B, R1-Distill-Qwen2.5-7B (Guo et al., 2025) and Qwen2.5-7B-Instruct (Team, 2024). We use 817 high-quality questions from the LIMO mathematical dataset (Ye et al., 2025) and evaluate both provided and self-generated CoT supervision. For self-generated supervision, we prompt R1-Distill-Qwen2.5-7B to generate 32 candidate responses per question and select the shortest correct response for training (as described in Sec. 3). We utilize provided higher-quality CoT supervision for R1-Distill-Qwen2.5-1.5B and R1-Distill-Qwen2.5-7B, and self-generated CoTs for Qwen2.5-7B-Instruct. We apply the same hyperparameter configurations of $\tau = 0.7$ and $\beta = 0.8$ to both sources of CoT supervision (as their hyperparameter search in

Figure 4: Change in correct answer confidence (Δ) across different segment types under varying τ . The red star marks the selected threshold τ^* .

Sec. 3.2 shows similar results). All models are fine-tuned with full parameters with a maximum sequence length of 16384. Additional training details are provided in Appendix C.3. We also provide model performance under different combination of τ and β in Appendix D.

Evaluation Details We conduct evaluation on both in-domain and out-of-domain benchmarks following the similar setup in (Ye et al., 2025). The in-domain benchmarks include Math500 (Hendrycks et al., 2021), AMC23, AIME24 and AIME25 while GPQA-Diamond (Rein et al., 2024), Minerva (Lewkowycz et al., 2022) and OlympiadBench (He et al., 2024) are out-of-domain. We report accuracy using greedy decoding, and pass@1 and pass@6 metrics using temperature sampling (temperature=0.6, top-p=1.0) as no universally optimal decoding strategy exists across all models and benchmarks. We employ a zero-shot chain-of-thought setting, with the maximum response length capped at 32,768 tokens. For larger benchmarks (MATH500, GPQA-Diamond, Minerva, and OlympiadBench), we sample 6 responses per instance, while for smaller benchmarks (AMC23 and AIME24), we sample 32 responses per instance. We compute the average token count across all sampled outputs as the response length.

4.2 MAIN RESULTS

Table 1 reports the overall comparison across six benchmarks. Relative to the baseline performance without SFT training, our segment-level selective SFT consistently outperforms full CoT SFT on both in-domain and out-of-domain datasets, across different baseline models and under both greedy decoding and temperature sampling. In addition, compared to full CoT SFT, our approach achieves a substantial reduction in token usage, leading to better optimization while simultaneously improving output efficiency. Notably, the gains in both accuracy and token reduction are more pronounced under greedy decoding. This is because the randomness in multiple temperature sampling tends to smooth out and partially offset the advantages of training. Nevertheless, even under such stochastic conditions, our approach still yields measurable improvements, underscoring its robust effectiveness.

Table 1: Comparison results on different baseline models. “Overall” reports the average accuracy under greedy decoding, or pass@1 and pass@6 under temperature sampling, together with the average output token count over all benchmarks. The percentages in parentheses indicate the relative accuracy improvement and token reduction of our method compared to full CoT SFT during generation. The best results are highlighted in **bold**.

Models	In Domain			Out of Domain			Acc./Pass@1	Pass@6	Overall
	MATH500	AMC23	AIME24	GPQA	Minerva	Olympiad			
<i>Greedy Decoding</i>									
R1-Distill-Qwen-1.5B	70.6	52.5	16.7	27.3	21.7	31.4	36.7	/	20244
Full CoT SFT	80.8	70.0	26.7	25.3	26.8	39.4	44.8	/	16520
Segment Selective SFT	82.4	60.0	40.0	28.8	27.6	42.8	46.9 (↑4.7%)	/	13506 (↓18.2%)
R1-Distill-Qwen-7B	85.8	85.0	46.7	42.9	38.2	47.9	57.7	/	12518
Full CoT SFT	91.2	90.0	50.0	42.4	41.2	57.9	62.1	/	9693
Segment Selective SFT	95.2	90.0	56.7	40.4	46.3	58.7	64.5 (↑3.9%)	/	8499 (↓12.3%)
Qwen2.5-7B-Instruct	77.0	50.0	10.0	38.9	34.9	37.5	41.4	/	1405
Full CoT SFT	77.2	55.0	23.3	38.9	29.8	40.9	44.2	/	10317
Segment Selective SFT	76.6	57.5	23.3	44.4	30.5	41.5	45.6 (↑3.2%)	/	9852 (↓4.5%)
<i>Temperature Sampling</i>									
R1-Distill-Qwen-1.5B	84.0	73.3	29.8	32.8	32.0	44.8	49.5	71.1	9791
Full CoT SFT	85.1	74.7	35.1	31.0	32.0	47.3	50.9	72.4	10043
Segment Selective SFT	85.1	75.9	36.1	32.8	31.9	48.1	51.7 (↑1.6%)	73.2 (↑1.1%)	9388 (↓6.5%)
R1-Distill-Qwen-7B	92.8	90.5	54.2	46.3	45.5	57.7	64.5	79.2	7593
Full CoT SFT	93.6	91.5	60.2	41.8	45.6	60.3	65.5	79.2	7934
Segment Selective SFT	93.3	91.9	61.0	42.3	45.8	60.3	65.8 (↑0.5%)	80.0 (↑1.0%)	7709 (↓2.8%)
Qwen2.5-7B-Instruct	75.7	51.9	12.0	36.9	35.4	37.2	41.5	60.2	910
Full CoT SFT	77.0	55.4	16.4	38.9	31.6	40.8	43.4	66.0	9902
Segment Selective SFT	77.1	58.5	16.4	43.7	32.4	41.9	45.0 (↑3.7%)	66.5 (↑0.8%)	9195 (↓7.1%)

4.3 ABLATION STUDY

To investigate the contributions of our important segment identification and selective SFT, we conduct an ablation study using R1-Distill-Qwen-1.5B with results averaged across datasets. Taking full CoT SFT as the baseline, we compare two categories *Pruned CoT SFT* according to our identified

378 important segments and *Selective SFT* using various criteria: (1) randomly selecting roughly 33%
 379 of segments from each CoT; (2) selecting the top 45% of tokens ranked by absolute IG values;
 380 (3) Selecting the top 45% of tokens ranked by original IG values; (4) Selecting only high-strength
 381 segments; (5) selecting segment with high strength and moderate direction consistency (our method).
 382 These ratios are chosen to ensure the amount of selected content is comparable across methods.

383 As shown in Table 2, pruning unimportant segments degrades accuracy, whereas our selective learning
 384 can improve SFT performance while reducing token usage. Among selective SFT, our IG-based
 385 important segments outperforms random segments and token-level selection based on ab-
 386 solute or original IG values, with absolute IG
 387 values proving more effective than original IGs
 388 for identifying importance. Furthermore, the
 389 improvement over only high-strength segments
 390 shows that incorporating moderate direction
 391 consistency can further filter out low-impacted
 392 segments to achieve greater token reduction without
 393 accuracy loss. Overall, these consistent improve-
 394 ments demonstrate that segment-level granular-
 395 ity better preserves reasoning coherence than
 396 token-level selection, and our IG-based strength-
 397 consistency criterion effectively identifies the
 398 most contributive reasoning components.

403 4.4 COMPARISON TO EXISTING SEGMENT IMPORTANCE MEASURES

404 To demonstrate the superiority of our IG-based importance segment identification, we apply Selective
 405 SFT using our identified segments and compare against alternative importance measures: (1) **First-
 406 Correct Solution** (Chen et al., 2024): retaining the first correct answer and all preceding segments
 407 as important; (2) **Confidence-Gain Segments** (Xu et al., 2025): identifying segments that directly
 408 improve the model’s confidence in the correct answer compared to when the segment is removed
 409 (as described in Sec. 3.1). (3) **Segment Perplexity** (Cui et al., 2025b): identifying critical segments
 410 whose removal leads to a substantial increase in CoT perplexity. (4) **Segment Entropy** Li et al.
 411 (2025a): prioritizing segments with higher aggregated token-level entropy as they indicate greater
 412 informational contribution. We set thresholds for methods (3) and (4) to ensure the selected important
 413 content occupies approximately the same 45~50% token ratio as our method for a fair comparison.

414 Results averaged across all datasets on R1-Distill-Qwen-1.5B are shown in Table 3. Our method
 415 consistently outperforms others in both accuracy and token reduction, demonstrating its abil-
 416 ity to more precisely identify segments that are truly contributive to reasoning, while perplex-
 417 ity and entropy are not entirely consistent signals of importance. The weak performance of
 418 Confidence-Gain Segments stems from its ne-
 419 glect of indirectly contributive segments, such
 420 as those supporting early-stage question under-
 421 standing or eliminating incorrect solution paths,
 422 as evident in its identification of only 24% of
 423 segments on average. Notably, our approach sur-
 424 passes First-Correct Solution, suggesting that
 425 segments beyond the first correct answer, such
 426 as answer verification or alternative solutions,
 427 are also meaningful by improving correct an-
 428 swer confidence. Moreover, it achieves greater
 429 token reduction than First-Correct Solution, indi-
 430 cating it can more selectively mask unnecessary
 431 segments before the first correct answer.

Table 2: Ablation study on R1-Distill-Qwen-1.5B. Our important segments have high attribution strength and moderate direction consistency.

Methods	Greedy		Sampling	
	Acc.	Length	Pass@1	Length
Full CoT SFT	44.8	16520	50.9	10043
Pruned CoT SFT	43.9	15097	49.2	7766
Selective SFT				
Random Segments	45.1	15138	50.8	10117
High-Abs-IG Tokens	46.1	14612	50.8	9495
High-Orig.-IG Tokens	45.2	14747	50.3	9876
High Strength Segments	46.9	14715	51.4	9466
Our Important Segments	46.9	13506	51.7	9388

Table 3: Selective SFT performance on important segments using different importance measures on R1-Distill-Qwen-1.5B. Accuracy and token length are averaged across all datasets.

Methods	Greedy		Sampling	
	Acc.	Length	Pass@1	Length
Full CoT SFT	44.8	16520	50.9	10043
First-Correct Solution	46.2	15238	51.0	9492
Confidence-Gain Segments	44.7	15479	50.3	9856
Segment Perplexity	44.7	14973	50.2	9816
Segment Entropy	44.5	16288	51.2	10148
IG-based Important Segments	46.9	13506	51.7	9388

432 4.5 PRUNING-BASED COMPARISON
433

434 We further apply our IG-based importance segment identification to segment-level CoT pruning
 435 for SFT, and compare against other strategies introduced in Sec. 4.4. We do not compare with
 436 token-level pruning methods as they would significantly disrupt text coherence and fluency in
 437 long CoTs and severely degrades SFT performance. We adjust thresholds for our method and
 438 compared methods (3) and (4) to prune nearly 30% of tokens from unimportant segments, as excessive
 439 pruning ratios substantially impact SFT performance. As shown in Table 4, our method better
 440 maintains performance in both decoding settings, compared to other CoT pruning strategies. Among
 441 them, First-Correct Solution performs best because it retains consecutive and complete reasoning
 442 processes, while other methods inevitably
 443 affect the information coherence of supervi-
 444 sions, leading to more severe performance
 445 drops and limited token reduction in long-
 446 CoT scenarios. However, performance still
 447 declines after First-Correct Solution prun-
 448 ing. Compared to Table 3, these results fur-
 449 ther demonstrate the effectiveness of our
 450 proposed segment-level selective learning
 451 across various importance metrics, which
 452 can maintain or even improve performance
 453 while reducing token consumption.

454
455 Table 4: Performance of different segment-level pruning
456 methods for CoT SFT on R1-Distill-Qwen-1.5B. Accu-
457 racy and token length are averaged across all datasets.

Methods	Greedy		Sampling	
	Acc.	Length	Pass@1	Length
Full CoT SFT	43.5	17140	50.7	10163
First-Correct Solution	45.2	11987	47.2	6846
Confidence-Gain Segments	40.3	11344	44.5	4180
Segment Perplexity	38.6	15892	47.9	8847
Segment Entropy	43.4	14321	45.9	7307
IG-based Important Segments	43.9	15097	49.2	7766

458 5 RELATED WORK
459

460 **LLMs Reasoning Efficiency** LLMs exhibit strong reasoning capabilities but typically generate
 461 verbose and redundant traces, leading to high computational costs and error accumulation (Sui et al.,
 462 2025; Wang et al., 2025a;d). Recent research explores various approaches to improve reasoning
 463 efficiency, which can be grouped into four categories. First, prompt-based methods design input
 464 prompts to control task difficulty and token budgets (Han et al., 2025; Renze & Guven, 2024). Second,
 465 decoding strategies dynamically reduce redundancy and shorten outputs during inference (Wang
 466 et al., 2025c; Liao et al., 2025). Third, latent reasoning approaches represent reasoning trajectories
 467 in latent spaces (Hao et al., 2024; Deng et al., 2024). Finally, training-based methods use SFT on
 468 compressed CoT supervision (Xia et al., 2025a; Lu et al., 2025) and reinforcement learning (RL) with
 469 conciseness rewards (Yuan et al., 2025; Lou et al., 2025). We focus on SFT-based methods, as they
 470 better balance efficiency and performance while serving as essential cold starts for RL-based training.

471 **Importance Measurement** To construct compressed CoT supervision for SFT-based methods, a key
 472 direction is to measure importance of different parts within full CoTs and prune less important content.
 473 Token-level methods typically utilize token logits and entropy to prioritize salient tokens but ignore
 474 semantic coherence (Xia et al., 2025a; Cheng et al., 2025; Wang et al., 2025b) Segment-level methods
 475 assess importance at segment granularity, better aligning with human reasoning units (Li et al., 2025a;
 476 Cui et al., 2025b). Moreover, Xu et al. (2025) propose leave-one-out and greedy forward selection
 477 to estimate segment attribution. Unlike these indirect measures, we use integrated gradients-based
 478 attribution method to quantify the direct contribution of each segments to final answer predictions.

479 **Selective Training** Recent research challenges traditional full sequence learning paradigm that
 480 uniformly optimizes loss on all tokens (Lai et al., 2024; Lin et al., 2025). Lin et al. (2024) selectively
 481 apply loss only to useful tokens and improve pretraining performance. Hans et al. (2024) propose
 482 training on randomly selected token prevents memorization without performance degradation. Kim
 483 et al. (2025) groups tokens in each sample by importance and optimizes weighted loss that adap-
 484 tively emphasizes challenging groups. In this work, we propose a segment-level selective learning
 485 framework that masks unimportant segments labeled by our importance measurement during SFT.

486 6 CONCLUSION
487

488 In this work, we proposed a segment-level selective learning framework for more effective learning
 489 from long reasoning traces. By incorporating integrated gradient attribution, we introduced two

486 segment-level metrics: *attribution strength* and *attribution direction consistency* to identify important
 487 segments with high strength but moderate consistency from full CoTs. Selective SFT on these
 488 segments improves both reasoning accuracy and reduces output length, outperforming full-CoT SFT.
 489 Our approach provides a principled way to identify critical reasoning segments and offers broader
 490 potential for emphasizing policy updates on targeted content in reinforcement learning.
 491

492 REPRODUCIBILITY STATEMENT

494 To support reproducibility, we provide detailed descriptions of our metrics and framework in Sec. 2
 495 and Appendix C.4. Additionally, we include comprehensive implementation details to reproduce our
 496 results in Sec. 4.1 and Appendix. C.3, covering hyperparameters selection, training and evaluation
 497 details, training frameworks. We will release our data and code after the anonymous review process.
 498

499 REFERENCES

501 Xingyu Chen, Jiahao Xu, Tian Liang, Zhiwei He, Jianhui Pang, Dian Yu, Linfeng Song, Qizhi Liu,
 502 Mengfei Zhou, Zhuosheng Zhang, et al. Do not think that much for $2+3=?$ on the overthinking of
 503 o1-like llms. *arXiv preprint arXiv:2412.21187*, 2024.

504 Daixuan Cheng, Shaohan Huang, Xuekai Zhu, Bo Dai, Wayne Xin Zhao, Zhenliang Zhang, and Furu
 505 Wei. Reasoning with exploration: An entropy perspective. *arXiv preprint arXiv:2506.14758*, 2025.

507 Yingqian Cui, Pengfei He, Jingying Zeng, Hui Liu, Xianfeng Tang, Zhenwei Dai, Yan Han, Chen
 508 Luo, Jing Huang, Zhen Li, Suhang Wang, Yue Xing, Jiliang Tang, and Qi He. Stepwise perplexity-
 509 guided refinement for efficient chain-of-thought reasoning in large language models, 2025a. URL
 510 <https://arxiv.org/abs/2502.13260>.

511 Yingqian Cui, Pengfei He, Jingying Zeng, Hui Liu, Xianfeng Tang, Zhenwei Dai, Yan Han, Chen Luo,
 512 Jing Huang, Zhen Li, et al. Stepwise perplexity-guided refinement for efficient chain-of-thought
 513 reasoning in large language models. *arXiv preprint arXiv:2502.13260*, 2025b.

515 Michael Han Daniel Han and Unsloth team. Unsloth, 2023. URL <http://github.com/unslothai/unsloth>.

517 Yuntian Deng, Yejin Choi, and Stuart Shieber. From explicit cot to implicit cot: Learning to internalize
 518 cot step by step, 2024. URL <https://arxiv.org/abs/2405.14838>.

520 Daya Guo, Dejian Yang, Haowei Zhang, Junxiao Song, Ruoyu Zhang, Runxin Xu, Qihao Zhu,
 521 Shirong Ma, Peiyi Wang, Xiao Bi, et al. Deepseek-r1: Incentivizing reasoning capability in llms
 522 via reinforcement learning. *arXiv preprint arXiv:2501.12948*, 2025.

523 Tingxu Han, Zhenting Wang, Chunrong Fang, Shiyu Zhao, Shiqing Ma, and Zhenyu Chen. Token-
 524 budget-aware llm reasoning, 2025. URL <https://arxiv.org/abs/2412.18547>.

526 Abhimanyu Hans, Yuxin Wen, Neel Jain, John Kirchenbauer, Hamid Kazemi, Prajwal Singhania,
 527 Siddharth Singh, Gowthami Somepalli, Jonas Geiping, Abhinav Bhatele, and Tom Goldstein.
 528 Be like a goldfish, don't memorize! mitigating memorization in generative llms, 2024. URL
 529 <https://arxiv.org/abs/2406.10209>.

530 Shibo Hao, Sainbayar Sukhbaatar, DiJia Su, Xian Li, Zhiting Hu, Jason Weston, and Yuandong
 531 Tian. Training large language models to reason in a continuous latent space, 2024. URL <https://arxiv.org/abs/2412.06769>.

533 Chaoqun He, Renjie Luo, Yuzhuo Bai, Shengding Hu, Zhen Leng Thai, Junhao Shen, Jinyi Hu,
 534 Xu Han, Yujie Huang, Yuxiang Zhang, et al. Olympiadbench: A challenging benchmark for
 535 promoting agi with olympiad-level bilingual multimodal scientific problems. *arXiv preprint
 536 arXiv:2402.14008*, 2024.

538 Dan Hendrycks, Collin Burns, Saurav Kadavath, Akul Arora, Steven Basart, Eric Tang, Dawn Song,
 539 and Jacob Steinhardt. Measuring mathematical problem solving with the math dataset. *arXiv
 540 preprint arXiv:2103.03874*, 2021.

540 Kerui Huang, Shuhan Liu, Xing Hu, Tongtong Xu, Lingfeng Bao, and Xin Xia. Reasoning efficiently
 541 through adaptive chain-of-thought compression: A self-optimizing framework, 2025. URL <https://arxiv.org/abs/2509.14093>.

542

543 Aaron Jaech, Adam Kalai, Adam Lerer, Adam Richardson, Ahmed El-Kishky, Aiden Low, Alec
 544 Helyar, Aleksander Madry, Alex Beutel, Alex Carney, et al. Openai o1 system card. *arXiv preprint*
 545 *arXiv:2412.16720*, 2024.

546

547 Gyuhak Kim, Sumiran Singh Thakur, Su Min Park, Wei Wei, and Yujia Bao. Sft-go: Supervised
 548 fine-tuning with group optimization for large language models. *arXiv preprint arXiv:2506.15021*,
 549 2025.

550

551 Xin Lai, Zhuotao Tian, Yukang Chen, Senqiao Yang, Xiangru Peng, and Jiaya Jia. Step-dpo: Step-
 552 wise preference optimization for long-chain reasoning of llms, 2024. URL <https://arxiv.org/abs/2406.18629>.

553

554 Aitor Lewkowycz, Anders Andreassen, David Dohan, Ethan Dyer, Henryk Michalewski, Vinay Ra-
 555 masesh, Ambrose Sloane, Cem Anil, Imanol Schlag, Theo Gutman-Solo, et al. Solving quantitative
 556 reasoning problems with language models. *Advances in neural information processing systems*,
 557 35:3843–3857, 2022.

558

559 Zeju Li, Jianyuan Zhong, Ziyang Zheng, Xiangyu Wen, Zhijian Xu, Yingying Cheng, Fan
 560 Zhang, and Qiang Xu. Compressing chain-of-thought in llms via step entropy. *arXiv preprint*
 561 *arXiv:2508.03346*, 2025a.

562

563 Zeju Li, Jianyuan Zhong, Ziyang Zheng, Xiangyu Wen, Zhijian Xu, Yingying Cheng, Fan Zhang,
 564 and Qiang Xu. Compressing chain-of-thought in llms via step entropy, 2025b. URL <https://arxiv.org/abs/2508.03346>.

565

566 Baohao Liao, Yuhui Xu, Hanze Dong, Junnan Li, Christof Monz, Silvio Savarese, Doyen Sahoo,
 567 and Caiming Xiong. Reward-guided speculative decoding for efficient llm reasoning, 2025. URL
 568 <https://arxiv.org/abs/2501.19324>.

569

570 Zhenghao Lin, Zhibin Gou, Yeyun Gong, Xiao Liu, Yelong Shen, Ruochen Xu, Chen Lin, Yujiu
 571 Yang, Jian Jiao, Nan Duan, et al. Rho-1: Not all tokens are what you need. *arXiv preprint*
 572 *arXiv:2404.07965*, 2024.

573

574 Zicheng Lin, Tian Liang, Jiahao Xu, Qiuwei Lin, Xing Wang, Ruilin Luo, Chufan Shi, Siheng Li,
 575 Yujiu Yang, and Zhaopeng Tu. Critical tokens matter: Token-level contrastive estimation enhances
 576 llm’s reasoning capability, 2025. URL <https://arxiv.org/abs/2411.19943>.

577

578 Chenwei Lou, Zewei Sun, Xinnian Liang, Meng Qu, Wei Shen, Wenqi Wang, Yuntao Li, Qingping
 579 Yang, and Shuangzhi Wu. Adacot: Pareto-optimal adaptive chain-of-thought triggering via
 580 reinforcement learning, 2025. URL <https://arxiv.org/abs/2505.11896>.

581

582 Ximing Lu, Seungju Han, David Acuna, Hyunwoo Kim, Jaehun Jung, Shrimai Prabhumoye, Niklas
 583 Muennighoff, Mostofa Patwary, Mohammad Shoeybi, Bryan Catanzaro, et al. Retro-search:
 584 Exploring untaken paths for deeper and efficient reasoning. *arXiv preprint arXiv:2504.04383*,
 585 2025.

586

587 Niklas Muennighoff, Zitong Yang, Weijia Shi, Xiang Lisa Li, Li Fei-Fei, Hannaneh Hajishirzi, Luke
 588 Zettlemoyer, Percy Liang, Emmanuel Candès, and Tatsunori Hashimoto. s1: Simple test-time
 589 scaling. *arXiv preprint arXiv:2501.19393*, 2025.

590

591 David Rein, Betty Li Hou, Asa Cooper Stickland, Jackson Petty, Richard Yuanzhe Pang, Julien Dirani,
 592 Julian Michael, and Samuel R Bowman. Gpqa: A graduate-level google-proof q&a benchmark. In
 593 *First Conference on Language Modeling*, 2024.

594

595 Matthew Renze and Erhan Guven. The benefits of a concise chain of thought on problem-solving in
 596 large language models. In *2024 2nd International Conference on Foundation and Large Language
 597 Models (FLLM)*, pp. 476–483. IEEE, November 2024. doi: 10.1109/fllm63129.2024.10852493.
 598 URL <http://dx.doi.org/10.1109/FLLM63129.2024.10852493>.

594 Yang Sui, Yu-Neng Chuang, Guanchu Wang, Jiamu Zhang, Tianyi Zhang, Jiayi Yuan, Hongyi Liu,
 595 Andrew Wen, Shaochen Zhong, Hanjie Chen, et al. Stop overthinking: A survey on efficient
 596 reasoning for large language models. *arXiv preprint arXiv:2503.16419*, 2025.

597

598 Mukund Sundararajan, Ankur Taly, and Qiqi Yan. Axiomatic attribution for deep networks. In
 599 *International conference on machine learning*, pp. 3319–3328. PMLR, 2017.

600 Qwen Team. Qwen2 technical report. *arXiv preprint arXiv:2407.10671*, 2024.

601

602 Rui Wang, Hongru Wang, Boyang Xue, Jianhui Pang, Shudong Liu, Yi Chen, Jiahao Qiu, Derek Fai
 603 Wong, Heng Ji, and Kam-Fai Wong. Harnessing the reasoning economy: A survey of efficient rea-
 604 soning for large language models, 2025a. URL <https://arxiv.org/abs/2503.24377>.

605 Shenzhi Wang, Le Yu, Chang Gao, Chujie Zheng, Shixuan Liu, Rui Lu, Kai Dang, Xionghui Chen,
 606 Jianxin Yang, Zhenru Zhang, et al. Beyond the 80/20 rule: High-entropy minority tokens drive
 607 effective reinforcement learning for llm reasoning. *arXiv preprint arXiv:2506.01939*, 2025b.

608

609 Siyuan Wang, Enda Zhao, Zhongyu Wei, and Xiang Ren. Stepwise informativeness search for efficient
 610 and effective llm reasoning, 2025c. URL <https://arxiv.org/abs/2502.15335>.

611

612 Yue Wang, Qiuzhi Liu, Jiahao Xu, Tian Liang, Xingyu Chen, Zhiwei He, Linfeng Song, Dian Yu,
 613 Juntao Li, Zhuseng Zhang, et al. Thoughts are all over the place: On the underthinking of
 614 o1-like llms. *arXiv preprint arXiv:2501.18585*, 2025d.

615

616 Jason Wei, Xuezhi Wang, Dale Schuurmans, Maarten Bosma, Fei Xia, Ed Chi, Quoc V Le, Denny
 617 Zhou, et al. Chain-of-thought prompting elicits reasoning in large language models. *Advances in
 618 neural information processing systems*, 35:24824–24837, 2022.

619

620 Yuyang Wu, Yifei Wang, Ziyu Ye, Tianqi Du, Stefanie Jegelka, and Yisen Wang. When more is
 621 less: Understanding chain-of-thought length in llms, 2025. URL <https://arxiv.org/abs/2502.07266>.

622

623 Heming Xia, Chak Tou Leong, Wenjie Wang, Yongqi Li, and Wenjie Li. Tokenskip: Controllable
 624 chain-of-thought compression in llms. *arXiv preprint arXiv:2502.12067*, 2025a.

625

626 Heming Xia, Chak Tou Leong, Wenjie Wang, Yongqi Li, and Wenjie Li. Tokenskip: Control-
 627 lable chain-of-thought compression in llms, 2025b. URL <https://arxiv.org/abs/2502.12067>.

628

629 Zhentao Xu, Fengyi Li, Albert Chen, and Xiaofeng Wang. Procut: Llm prompt compression via
 630 attribution estimation, 2025. URL <https://arxiv.org/abs/2508.02053>.

631

632 An Yang, Anfeng Li, Baosong Yang, Beichen Zhang, Binyuan Hui, Bo Zheng, Bowen Yu, Chang
 633 Gao, Chengan Huang, Chenxu Lv, et al. Qwen3 technical report. *arXiv preprint arXiv:2505.09388*,
 634 2025.

635

636 Yixin Ye, Zhen Huang, Yang Xiao, Ethan Chern, Shijie Xia, and Pengfei Liu. Limo: Less is more for
 637 reasoning. *arXiv preprint arXiv:2502.03387*, 2025.

638

639 Danlong Yuan, Tian Xie, Shaohan Huang, Zhuocheng Gong, Huishuai Zhang, Chong Luo, Furu Wei,
 640 and Dongyan Zhao. Efficient rl training for reasoning models via length-aware optimization, 2025.
 641 URL <https://arxiv.org/abs/2505.12284>.

642

643

644

645

646

647

648 A POSITIONAL DISTRIBUTIONAL OF SEGMENTS IMPORTANCE
649

650 We analyze the positional distribution of segment importance within long CoTs by identifying the
 651 decision segment, defined as the first segment that derives the correct answer. We observe 40%
 652 of important segments appear after the decision segment, indicating that additional verification
 653 or exploration beyond the initial correct answer can still play a crucial role. In contrast, 57% of
 654 unimportant segments occur before the decision segment, suggesting that the search for the correct
 655 answer often involves redundant behaviors such as repetition and truncation. This also highlights
 656 that simply splitting by decision segments may introduce a considerable number of false positives
 657 and false negatives (Wang et al., 2025d). A finer-grained analysis further reveals that most low-
 658 strength unimportant segments (64%) occur before the decision segment. In contrast, the majority
 659 of high-consistency unimportant segments (72%) appear after it. **Combined with Figure 3.1 shows**
 660 **that high-consistency segments typically induce minimal improvement in correct-answer confidence,**
 661 **this suggests that once the correct answer is found, such segments are prone to shallow or redundant**
 662 **elaboration as formalized verification or reinforcement of the already-found answer rather than**
 663 **introducing deeper critical examination.**

664 B INCOMPLETELY TRUNCATED SEGMENT IDENTIFICATION
665

666 To determine whether a given segment is complete or truncated by alternative content, we employ
 667 Qwen3-8B with a carefully designed prompt template. The template, shown in Table 5, describes the
 668 task and includes few-shot examples. It instructs the model to first reason step by step in thinking
 669 mode, and then output a final judgment on whether Segment 2, given the surrounding context of
 670 Segment 1 and Segment 3, is a truncated segment. We frame this as a 0/1 classification task rather
 671 than using Yes/No answers, since we find that restricting the output to binary digits yields more
 672 reliable performance.

673 For each segment, we conduct up to two inference rounds. In round 1, the model runs in thinking
 674 mode with a token budget of 2000, temperature 0.2, top_p 0.7, and repetition_penalty 1.1. If the
 675 model fails to reach to a conclusion in this round, we will inject an **Early-Stopping Prompt** (as
 676 shown in Table 6), and run the model in round 2, with temperature 0.1, top_p 0.7, max_tokens 1000,
 677 and repetition_penalty 1.1. The input for round 2 consists of the original input and the Round 1
 678 output, followed by the injected Early-Stopping Prompt.

680 C SUPPLEMENTARY IMPLEMENTATION DETAILS
681682 C.1 LLM USAGE
683

684 Our use of LLMs in this paper comprises two main components: writing assistance and tools for
 685 data analysis and construction. During writing, we utilize ChatGPT 5 and Claude Sonnet 4 to help
 686 polish the exposition. For data analysis and construction, as described in Section 4.1, we employ
 687 R1-Distill-Qwen2.5-7B to generate its CoT trajectories leading to correct answers as supervision for
 688 SFT, and to compute integrated gradient attributions on each token.

689 C.2 SEGMENTATION KEYWORDS
690

691 To partition each long CoT into individual segments, we select transition keywords following (Lu
 692 et al., 2025) which includes “But”, “Wait”, “Alternatively”, “However”, “Hmm”, “Hmmm”, “Not
 693 sure”, “Going back”, “Backtrack”, “Trace back”, and “Another”. Specifically, most of our keywords
 694 are directly adopted from (Lu et al., 2025), including “\n\nWait”, “\n\nAlternatively”, “\n\nHowever”,
 695 “\n\nNot sure”, “\n\nGoing back”, “\n\nBacktrack”, “\n\nTrace back”, “\n\nAnother”. We prepend
 696 “\n\n” to each keyword because many LRMAs naturally structure their reasoning output with paragraph
 697 breaks, making this prefix a reliable delimiter for identifying reasoning segments. Our keywords
 698 differ from Lu et al. (2025) in two ways. First, instead of the broad keyword “But”, we use more
 699 specific variants including “\n\nBut wait”, “\n\nBut alternatively” and “\n\nBut just to”. This change
 700 is motivated by empirical observations that LRMAs, especially smaller distilled models like R1-Distill-
 701 Qwen2.5-7B, tend to use “But” as conversational fillers rather than a meaningful reasoning transition.
 Second, we exclude fillers such as “Hmm” and “Hmmm”, which we also find to be frequently

756 used as verbal habits instead of genuine segment boundaries. These design choices aim to balance
 757 generalizability across LRMs while ensuring that segmented reasoning units are meaningful rather
 758 than overly fragmented.

759 To illustrate the effectiveness of our method using different keywords, we also experiment with using
 760 the exact keyword list from (Lu et al., 2025). We apply these keywords to segment the original
 761 LIMO CoTs and retrain R1-Distill-Qwen2.5-1.5B. This results in much finer-grained segmentation,
 762 increasing the average number of segments from 22.5 to 33.5 per reasoning trace. The selective SFT
 763 results in Table 7 show that this finer segmentation leads to higher accuracy and more concise outputs.
 764 We attribute this to that LIMO traces are generated by higher-quality models (e.g., DeepSeek-R1,
 765 QwQ-32B), whose reasoning contains fewer meaningless fillers. In such cases, finer segmentation
 766 yields more precise identification of important reasoning units.

767
 768 Table 7: Results on R1-Distill-Qwen-1.5B using new transition keywords from (Lu et al., 2025).

Methods	Greedy		Sampling	
	Acc.	Length	Pass@1	Length
R1-Distill-Qwen-1.5B	36.7	20244	49.5	9791
Full CoT SFT	44.8	16520	50.9	10043
Segment Selective SFT (Original Keywords)	46.9	13506	51.7	9388
Segment Selective SFT (New Keywords)	51.5	12646	51.5	9167

775 776 C.3 TRAINING & EVALUATION DETAILS

777 All models are trained using the Unslloth training framework (Daniel Han & team, 2023). Specifically,
 778 we train R1-Distill-Qwen2.5-1.5B and R1-Distill-Qwen2.5-7B for 10 epochs respectively with a
 779 learning rate of 3e-5 and 1.5e-5. For Qwen2.5-7B-Instruct which does not original support long-chain
 780 reasoning, we adopt a two-stage SFT strategy that first conducts full CoT training for 7 epochs with
 781 a learning rate of 1.5e-5, and continued training for 4 additional epochs using only the identified
 782 important segments, with a learning rate of 8e-6. For a fair comparison, the full CoT SFT baseline is
 783 trained with the same two-stage schedule. All experiments employ a cosine learning rate schedule.
 784 The overall performance (including greedy accuracy, sampling pass@1, pass@6 and output length)
 785 reported in this paper is calculated using macro averaging across all datasets, treating each dataset as
 786 equally important.

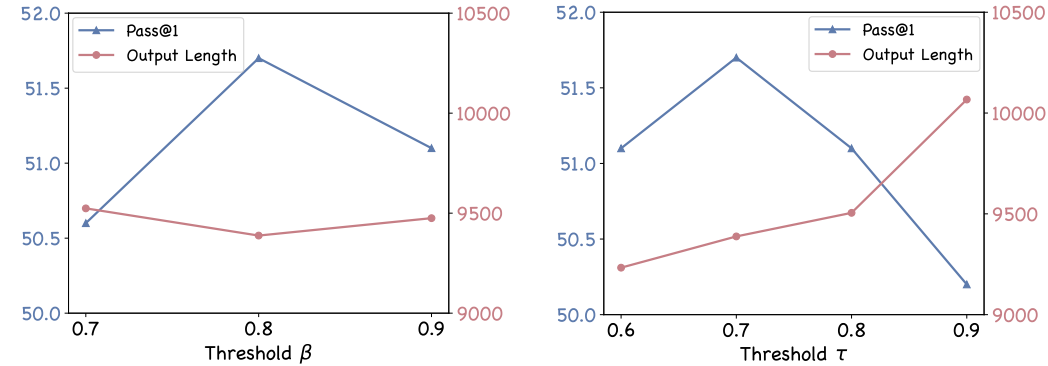
787 788 C.4 METHODOLOGY DETAILS

789 For calculating token-level integrated gradients, we use $J = 50$ interpolation steps to estimate
 790 the integral in the IG computation **for the cost-precision trade-off as indicated by** (Sundararajan
 791 et al., 2017) **that 20~300 integration steps typically approximate the path integral within about 5%**
 792 **approximation error.** We specifically utilize R1-Distill-Qwen2.5-7B to calculate token IG values on
 793 both reference long CoTs provided by the LIMO dataset and self-generated long CoT supervisions by
 794 Distill-Qwen2.5-7B. **Each costs roughly 7 (GPU×hours), compared to the 8 (GPU×hours) required**
 795 **for a full SFT run of the same 7B model.** In deploying our method and all baselines, we additionally
 796 include the first and last segments which are responsible for establishing the problem understanding
 797 and for explicitly formatting the final answer, together with the identified important segments as
 798 learning objectives in both selective SFT and pruning-based settings. For segment-level aggregation,
 799 we have explored several strategies: (1) length-normalized summation, (2) direct summation, and (3)
 800 averaging the top 20% of token IG values. We find that the first two achieve comparable performance,
 801 while length-normalized summation better mitigates bias toward longer segments.

802 803 D DIFFERENT THRESHOLD HYPERPARAMETERS

804 We further experiment with different selection of the hyperparameters τ and β on R1-Distill-
 805 Qwen2.5-1.5B. We first explore different values of $\beta \in \{0.7, 0.8, 0.9\}$ under a fixed $\tau = 0.7$ and
 806 report the temperature sampling results in the left panel of Figure 5. We observe that $\beta = 0.8$ achieves
 807 the best performance, which is also adopted as the main experimental setting in our paper. Based on
 808 $\beta = 0.8$, we further validate whether $\tau = 0.7$ indeed achieves the best experimental performance as
 809 expected in our hyperparameter search. We vary $\tau \in \{0.6, 0.7, 0.8, 0.9\}$ as shown in the right panel

of Figure 5. Results show that as τ increases, more segments are selected as important among all candidates. Consequently, the token reduction after training becomes smaller. However, performance decreases because higher τ introduces more false positives, and a denser loss mask negatively impacts training. Overall, $\tau = 0.7$ and $\beta = 0.8$ constitute our final experimental setting.

Figure 5: Model performance under different hyperparameters τ and β .

E ADDITIONAL RESULTS ON LLAMA3.1-8B-INSTRUCT.

To further demonstrate the effectiveness of our method beyond the Qwen model family, we additionally train LLama3.1-8B-Instruct using the LIMO dataset. As shown in Table 8, Segment Selective SFT still achieves performance improvement, demonstrating that our method generalizes well to a different model family.

Table 8: Comparison results on LLaMA3.1-8B-Instruct.

Methods	Greedy		Sampling	
	Acc.	Length	Pass@1	Length
LLaMA3.1-8B-Instruct	24.0	9691	23.5	4161
Full CoT SFT	30.4	17474	33.0	15067
Segment Selective SFT	33.8	16005	33.5	14669